JOURNAL OF CATALYSIS 116, 309–317 (1989)

The Preparation of WO_3/TiO_2 and WO_3/Al_2O_3 and Characterization by Temperature-Programmed Reduction

DIRK C. VERMAIRE[1] AND PIETER C. VAN BERGE

Department of Chemistry, Rand Afrikaans University, P.O. Box 524, Johannesburg 2000, South Africa

Received May 6, 1988; revised October 24, 1988

An equilibrium adsorption technique was used to prepare WO_3/TiO_2 and WO_3/Al_2O_3 samples. The tungsten loading could be controlled by varying the pH and concentration of the aqueous solutions. For both supports there was a definite maximum to the amount of tungsten that adsorbed spontaneously, viz. 988 ± 21 and 669 ± 19 μmol per 100 m^2 for alumina and titania, respectively. The hydroxyl group to tungsten ratio was 2:1 on alumina for a fully hydroxylated surface. On titania the ratio was 1:1, based on the reacting hydroxyl group density. These stoichiometries point to a very specific interaction between the tungstate ions and the hydroxyl groups on the support surface during adsorption. Unlike on alumina, the reduction of tungsten oxide on titania (anatase) takes place in two well-separated steps viz., $W^{6+} \rightarrow W^{4+} \rightarrow W^0$. During reduction the titania is transformed from anatase to rutile which has the same crystal structure and metal to oxygen bond length as WO_2 and can thus facilitate and stabilize the W^{4+} ions. A stepwise reduction of tungsten oxide was not observed on alumina, probably due to the inability of alumina to stabilize the intermediate oxidation states of tungsten.

INTRODUCTION

The adsorption of metal oxyanions from aqueous solutions onto alumina, titania, and other oxide supports has been explained in terms of the isoelectric points (iep) of these oxides (*1, 2*). A pH below or above that of the iep causes the surface hydroxyl groups to be either protonated or deprotonated, giving the surface a positive charge or negative charge, respectively. The observed increase in the adsorption of metal oxyanions from solution at a pH below that of the iep of the supports has consequently been explained in terms of an electrostatic attraction between the negative ions and the positive surface. This concept explains the observed adsorption of anions on different supports around the iep very well. In line with this Wang and Hall (*3*) showed that the adsorption of transition metal ions onto alumina increased considerably when the pH was lowered to below that of the iep of alumina ($6.0 < \text{iep} < 8.0$). It was also found, for the adsorption of molybdenum, that lowering the pH to 2.0 resulted in a second increase in molybdenum adsorption. The reason for this increase was not addressed.

WO_3/Al_2O_3 (*4–6*) and WO_3/TiO_2 (*7*) have previously been characterized with laser Raman spectroscopy. Below monolayer coverages the tungsten oxide was found to be present as a highly dispersed surface oxide species bound to the support surface. Salvati *et al.* (*5*) proposed that on alumina, the WO_x exists as a tetrahedral WO_4^{2-} that interacts with the surface. This picture was recently confirmed by X-ray absorption near edge spectroscopy (*8*).

The reduction behavior of WO_3/Al_2O_3 has been studied with temperature-programmed reduction (tpr) (*9, 10*) and X-ray photoelectron spectroscopy (XPS) (*5, 11, 12*). It was found that, at monolayer coverages and less, the strong interaction between the tungsten oxide and the alumina substantially suppressed its reducibility. XPS showed that the tungsten (W^{6+}) re-

[1] Present address: Sasol Technology (Pty), P.O. Box 1, Sasolburg, 9570, South Africa.

0021-9517/89 $3.00

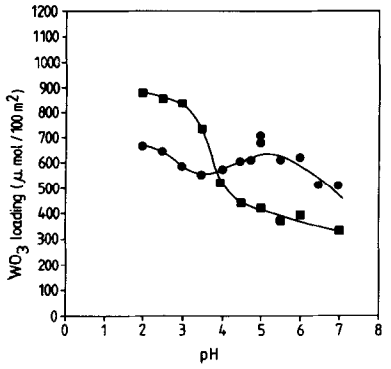

FIG. 1. The effect of pH of the tungsten solution on the tungsten loading. (■) Alumina, $[WO_4^{2-}]_0 = 2.95 \times 10^{-3}$ mol dm^{-3}; (●) titania, $[WO_4^{2-}]_0 = 2.80 \times 10^{-3}$ mol dm^{-3}. $[WO_4^{2-}]_0$ is the starting concentration of monotungstate.

duced directly to W^0, and not via its intermediate oxidation states (W^{5+}, W^{4+}, and W^{2+}), as is the case for pure WO_3 (*11, 12*). The reduction behavior of WO_3/TiO_2 has been studied by tpr, but not in depth (*13*).

In this work, WO_3/Al_2O_3 and WO_3/TiO_2 were prepared by an equilibrium adsorption technique. It was found that the observed adsorption behavior of tungsten on alumina and on titania, at pH values well below the ieps of the supports, could not be explained by electrostatic adsorption alone. A combined electrostatic adsorption/chemisorption mechanism is proposed. Laser Raman spectroscopy and tpr were used to characterize the systems.

METHODS

The samples were prepared by an equilibrium adsorption technique. The tungstate solution was circulated from a polyethylene reservoir via a glass adsorption cell, containing 3 g of support material, back into the reservoir. The adsorption time was 25 h in all cases. The pH of the solution in the reservoir was maintained by addition of either NH_4OH or HNO_3. The supports were aluminum oxide C and titanium dioxide P25, both from Degussa. Prior to loading into the adsorption cell both supports were pelletized (60 kg cm^{-2}), crushed, and sieved to a particle size of between 0.180 and 0.131 mm. This was then washed with deionized water to remove any loose material.

The tungstate solutions were prepared with ammonium paratungstate ($NH_4W_{20}O_{60}$ from Fluka) and analyzed with atomic absorption spectroscopy (Varian AA 875). After adsorption the samples were dried at 150°C and analyzed with X-ray fluorescence (EDAX Model 711 and 902D).

X-ray diffraction powder analyses were carried out on a standard Philips X-ray diffractometer using Cu$K\alpha$ radiation.

The Raman spectra were recorded on a Coderg spectrometer equipped with an argon ion laser. The output power of the laser was 400 mW (514.5 nm). The Raman spectra of the samples were recorded after calcination at 500°C for 16 h.

The temperature-programmed reduction equipment consisted of a sorptometer (Perkin–Elmer Model 212D) connected to a reduction cell plus furnace and a cold trap. The sorptometer was used to mix the reducing gas (10.0% H_2 in Ar) and to control the flow (28.2 ml_{stp} min^{-1}). The hydrogen concentration after the reduction cell was monitored with the thermal conductivity detector of the sorptometer, and the signal was recorded on an X–Y recorder (JJ Instruments Model PL 1500). The furnace was controlled by a temperature programmer (RKC Model PS-962 C), and the temperature could be increased linearly from room temperature to 1500 K. The temperature inside the reduction cell was monitored with a type-K thermocouple.

RESULTS

(*a*) *Sample Preparation*

The effect of the pH of the tungstate solution on the loading after 25 h adsorption is shown in Fig. 1. The pH could not be taken lower than 2.0, due to the precipitation of tungstic acid at these low values. Figure 1 shows that the tungsten loading of the two supports is clearly dependent on the pH of the solution, and that the supports differ

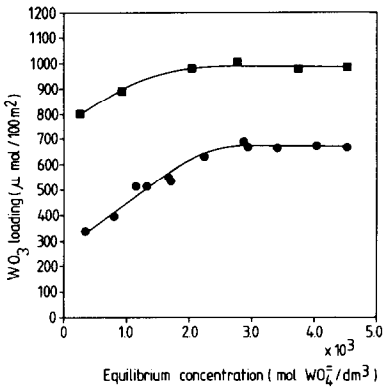

FIG. 2. The effect of concentration on tungsten loading at pH 2.0 (■, alumina; ● titania).

considerably in their adsorption behavior. On alumina there is a strong increase in adsorption below a pH of 4, followed by a leveling off below a pH of 3.0. The tungsten loading on titania already levels off at a pH of 5.0 and is overall much less pH dependent at lower values.

Figure 2 shows that the tungsten loading is also affected by the concentration, but only when the final concentration is less than 2.0×10^{-3} mol WO_4^{2-} dm^{-3}. This cutoff point is the same for both supports. Table 1 presents the maximum surface loading of tungsten oxide that was obtained on these two supports and the area per WO_3 molecule at that coverage. The maximum surface loading obtained under these conditions will be referred to as a monolayer, although it will become clear that this is strictly speaking not the case. It follows from Table 1 that tungsten packs more densely on alumina than on titania. The 0.17 nm^2 obtained for the area of a WO_3 molecule on alumina is the same as that calculated for a single layer of WO_3 in pure tungsten trioxide.

(*b*) *Raman Spectroscopy*

WO_3/Al_2O_3. The alumina itself showed two broad Raman bands of low intensity, at 569 and 1093 cm^{-1}, in the range 100 to 1600 cm^{-1}. For the monolayer WO_3/Al_2O_3 after calcination, three additional Raman bands were observed at 716, 809, and 986 cm^{-1}. The Raman bands at 809 and 716 cm^{-1} were of very low and low intensity, respectively, compared to the Raman band at 986 cm^{-1}. These two bands compare well with the Raman bands for WO_3 at 808 and 715 cm^{-1} and are indicative of small WO_3 crystallites. The Raman band at 986 cm^{-1} has been assigned to the symmetrical stretching mode (W=O) of an amorphous tetrahedrally coordinated tungsten species, covering most of the alumina surface (*5, 8, 14*). A calcined 0.42 monolayer WO_3/Al_2O_3 sample exhibited only the Raman band at 986 cm^{-1}.

WO_3/TiO_2. The major Raman bands for titania are all below 700 cm^{-1}. The monolayer WO_3/TiO_2 sample exhibited, after calcination, only one Raman band that could be assigned to tungsten oxide at 977 cm^{-1}. As on alumina, this band has been assigned to the symmetrical stretching mode of an amorphous tungsten species (WO_x) on the surface (*7*). By analogy with WO_3/Al_2O_3 it may be assumed that the WO_x on titania also has a tetrahedral coordination. The Raman spectrum of a calcined 0.76 monolayer sample was the same as that for the complete monolayer WO_3/TiO_2.

TABLE 1

Maximum Tungsten Trioxide Loading on Alumina and Titania Supports

Support	BET area (m^2 g^{-1})	Tungsten trioxide loading		Area/WO_3 molecule (nm^2)
		(mass%)	(μmol m^{-2})	
Al_2O_3	90	17.1 ± 0.3	(988 ± 21) × 10^{-2}	0.168 ± 0.003
TiO_2	50	7.2 ± 0.2	(669 ± 19) × 10^{-2}	0.248 ± 0.004

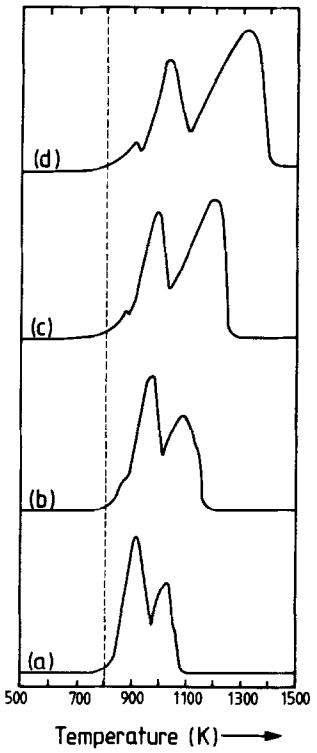

FIG. 3. Temperature-programmed reduction profiles (10 K min^{-1}) of WO_3 as a function of sample size. (a) 10 mg; (b) 20 mg; (c) 52 mg; (d) 103 mg.

(c) *Temperature-Programmed Reduction*

Figure 3 presents the tpr profiles of pure WO_3 as a function of sample size. For the 103-mg sample three reduction maxima were observed at 911, 1038, and 1303 K, respectively. A decrease in the sample size caused the maxima to move closer together and to shift to lower temperatures. For the 10-mg sample only two maxima, at 929 and 1036 K, remained.

The reduction of tungsten trioxide proceeds as (*15*).

$$\underset{\text{I}}{WO_3} \rightarrow \underset{\text{II}}{W_{20}O_{58}} \rightarrow \underset{\text{III}}{WO_2} \rightarrow W \qquad (1)$$

The percentage of oxygen removed with transitions I, II, and III is 3.3, 30.0, and 66.7%, respectively. The values obtained from the areas under the reduction peaks in the reduction profiles of the 103-mg sample are approximately 5, 27, and 68%. This is in good agreement with the reduction of WO_3 according to Eq. (1) and was further confirmed by XRD analyses.

The different reduction steps are well resolved for a 100-mg sample, and this made it possible to determine the energy of activation (E_a) for each reduction step, by using the equation (*16*)

$$2 \ln T_m - \ln \beta + p \ln[H_2]_m + (1 - q) \ln[\text{Solid}]^q = E_a/RT_m + \ln(E_a/RA) \qquad (2)$$

T_m represents the temperature at maximum rate (K), β is the heating rate (K min^{-1}), $[H_2]_m$ is the hydrogen concentration at T_m (mol dm^{-3}), R is the gas constant (J mol^{-1} K^{-1}), and A is the Arrhenius constant (min dm^3 mol^{-1}). The reaction order (q) with respect to the reducing solid was taken to be one, as was the reaction order (p) with respect to the hydrogen concentration (*16*). Figure 4 shows the activation energy plots for each reduction. The activation energies and preexponential factors are given in Table 2. Three different temperature gradients (β = 1.8, 9.2, and 30.9 K min^{-1}) were used in each case.

Figure 5 presents the tpr profiles for the supported tungsten oxides, as well as the tpr profile for titania. The γ-alumina showed no reduction up to 1450 K. The monolayer WO_3/Al_2O_3 sample shows two

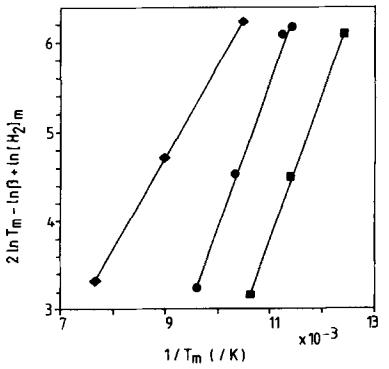

FIG. 4. Activation energy plots for the reduction of WO_3. (■) $WO_3 \rightarrow W_{20}O_{58}$; (●) $W_{20}O_{58} \rightarrow WO_2$; (◆) $WO_2 \rightarrow W$.

TABLE 2

Energies of Activation for the Reduction of Pure WO_3 and Supported on TiO_2

Transition	E_a (kJ mol^{-1})	A (min dm^3 mol^{-1})
Pure		
$WO_3 \rightarrow W_{20}O_{58}$	134 ± 4	1.75×10^{10}
$WO_{20}O_{58} \rightarrow WO_2$	136 ± 10	4.09×10^{9}
$WO_2 \rightarrow W$	84 ± 1	8.68×10^{5}
Supported on TiO_2		
$WO_3 \rightarrow WO_2$	272 ± 16	2.03×10^{17}

reduction maxima at 1108 and 1336 K, respectively, but the 0.42 monolayer catalyst shows only one reduction maximum at 1330 K. The absence of the 1108 K reduction maximum for the 0.42 monolayer sample indicates that the double maximum in the monolayer sample is due to the reduction of two different tungsten oxide species and not to a two-step reduction of the supported tungsten oxide. The monolayer WO_3/TiO_2 sample shows three reduction maxima, at 655, 1017, and 1248 K, respectively. The maximum at 655 K is not observed for the 0.76 monolayer sample, and this points again to the existence of two different tungsten oxide species on the monolayer sample. The two large maxima, at 1017 and 1248 K, are also present on the 0.76 monolayer sample and indicate a two-step reduction for the bulk of the supported tungsten oxide. Titania itself also undergoes reduction, and the XRD pattern of a sample quenched at 1000 K further showed that the anatase had been transformed to rutile in the heating process. The reduction profile of TiO_2 partially obscures that of the supported tungsten oxide, but by a proportional subtraction of the titania profile from that of the monolayer sample, the reduction profile of the supported tungsten oxide is obtained (dashed line). A quantitative analysis of the 1017 K reduction maximum further shows that it corresponds to 32 ± 2% of the oxygen that is associated with the supported tungsten (W^{6+}). The 1017 K maximum could thus be due to the reduction of W^{6+} to W^{4+}. The activation energy plot for this reduction is given in Fig. 6. A quantitative analysis of the 1248 K maximum indicates that it represents approximately 46% of the oxygen associated with the W^{6+}. If the reduction of W^{6+} to W^{4+} was complete, this is equivalent to 68% of the oxygen associated with W^{4+}. This means that at 1500 K approximately 32% of the tungsten is still present at W^{4+}.

DISCUSSION

The average of the calculated hydroxyl group density for the low index planes of

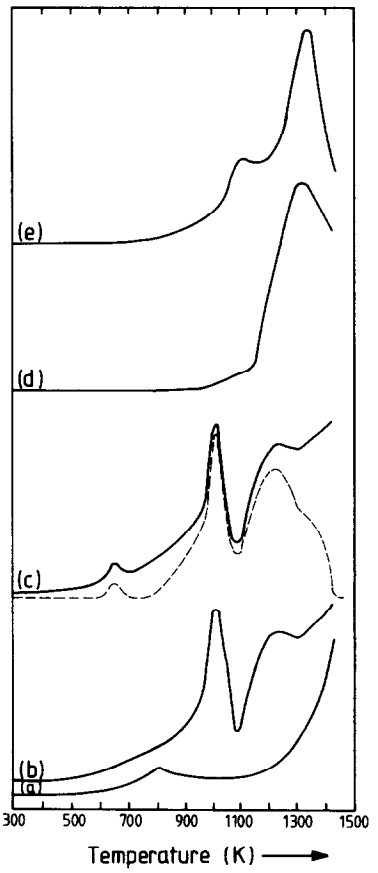

FIG. 5. Temperature-programmed reduction profiles (10 K min^{-1}) for WO_3/Al_2O_3, WO_3/TiO_2, and TiO_2. (a) TiO_2; (b) 0.72 monolayer WO_3/TiO_2; (c) monolayer WO_3/TiO_2; (d) 0.42 monolayer WO_3/Al_2O_3; (e) monolayer WO_3/Al_2O_3.

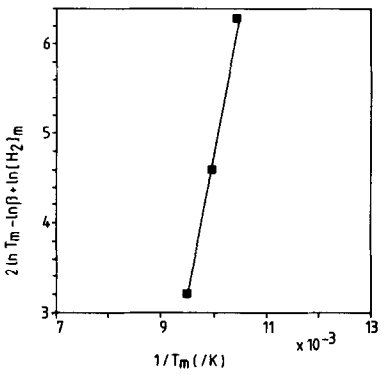

FIG. 6. Activation energy plot for the reduction of WO_3/TiO_2 to WO_2/TiO_2. (β = 1.8, 9.2, and 30.9 K min^{-1})

alumina is 12.0 OH nm^{-2} (*17*). The surface density of tungsten trioxide on alumina at maximum coverage is 6.0 WO_3 nm^{-2}. This points to a stoichiometry of 1 to 2 between the tungsten oxide and the hydroxyl groups on alumina. For anatase titania the estimated surface density for a fully hydroxylated surface is 12 to 14 OH nm^{-2}, and the number of reacting hydroxyl groups on anatase (Degussa P25) was found to be approximately 4.3 OH nm^{-2} (*18*). The surface density of tungsten trioxide on this support at maximum coverage is 4.0 WO_3 nm^{-2}, pointing to a 1 to 1 stoichiometry between the tungsten oxide and the reacting hydroxyl groups. These stoichiometries point to a specific interaction between the tungstate ions and the surface hydroxyl groups.

The tungstate species that are present in aqueous solutions depend on the pH of the solution (*19, 20*). At a pH of between 3.2 and 6.2 the initial tungstate in solution is paratungstate A ($[W_7O_{24}]^{6-}$) which is slowly transformed into paratungstate B ($[W_{12}O_{42}H_2]^{10-}$). At pH values of between 3.2 and 1.0 a metatungstate ($[(H_2)W_{12}O_{40}]^{6-}$) is present. The tungsten atom to charge ratio is approximately 1.2 for the paratungstates and 2.0 for the metatungstates. If the adsorption of anions is purely electrostatic, a 67% increase in tungsten loading is expected at a pH of around 3.2. Such a change is observed at a pH of between 3.0 and 4.0 on alumina, but not on titania.

Similarly, adsorption at a pH of 2.0 ($[(H_2)W_{12}O_{40}]^{6-}$ adsorbing) should yield a hydroxyl group to tungsten atom ratio of 1 : 2 on both supports. This is, however, not the case. From the above it can be inferred that electrostatic attraction alone cannot explain the observed tungsten to hydroxyl group ratios. In order to explain these, a chemical reaction between the polytungstates and the surface hydroxyl groups, at pH values below the ieps of the supports, must be accepted. Initial attraction of the polytungstate ions to the oxide surface is electrostatic.

The 1 : 2 stoichiometry on alumina can be explained by assuming a decomposition of the polytungstates on the surface and the formation of a surface complex (Scheme 3), as was first proposed by Ng and Hercules during calcination of the catalyst (*2*). The 1 : 2 adsorption stoichiometry points, however, to the possibility that such a complex may already be formed during the adsorption process.

The 1 : 1 ratio found for titania does not appear to fit the formation of a similar complex. A density of 4.3 for the reacting hydroxyl groups on titania means that these are on average 0.54 nm apart. Taking the W–O bond length in tungstates and oxides to be approximately 0.20 nm (*19, 21*), it would be impossible for the tetrahedral monotungstate to span two of these hydroxyl groups. This is thus in agreement with the observed 1 : 1 stoichiometry, and the formation of a surface complex upon adsorption as in Scheme 3 is not possible. However, two types of hydroxyl groups exist on the titania surface, viz. terminally and bridged bonded groups (*22, 23*). The 1 : 1 stoichiometry can thus be explained by

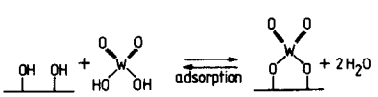

SCHEME 3

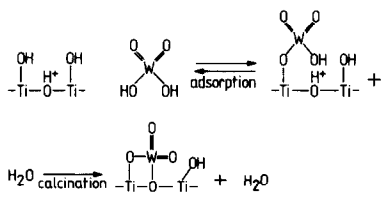

SCHEME 4

an initial replacement of the terminal hydroxyl groups by monotungstate during adsorption and a subsequent reaction with the adjacent bridged hydroxyl group upon calcination [Scheme 4].

It is clear that a reaction with, or displacement of, the hydroxyl groups by monotungstates can explain the observed hydroxyl group to tungsten atom stoichiometries, and thereby also the fact that there is a definite maximum to the amount of tungsten that can be adsorbed onto alumina or titania. In this adsorption mechanism the observed sharp increase in the tungsten adsorption on alumina at a pH between 4.0 and 3.0 is interpreted as the point where the adsorption changes from electrostatic adsorption to chemical adsorption. This transition in adsorption mechanism cannot be seen clearly on titania.

Previous work with Raman spectroscopy has confirmed the presence of tetrahedrally coordinated tungsten at monolayer coverage and less on alumina (*4–6*), and the indications are that it exists in the same form on titania (*7*). The Raman results in our work are in agreement with this and support the proposed adsorption mechanism in that it also results in the formation of tetrahedrally coordinated tungsten oxides.

The shifts in the reduction peak maxima to lower temperatures with decreasing sample size for the reduction of WO_3 can be influenced by one of the following two factors, or a combination thereof: (a) A kinetic effect due to an increased hydrogen concentration at peak maximum with decreasing sample size (by reducing the sample size from 103 to 20 mg, the hydrogen concentration at peak maximum for II and III increased by 47 and 92%, respectively). (b) A decrease of the H_2O partial pressure within the sample bed with decreasing sample size. H_2O was found to inhibit the reduction of MoO_3 (*24*), due to either fast reoxidation of reduced Mo ions or to H_2O catalyzing surface reconstruction. Similar effects could play a role in the reduction of WO_3. In the calculations of the energies of activation for the different reduction steps, the former is accounted for, but the latter will affect the accuracy of the obtained values.

Reduction step I in Eq. (1) corresponds to the reduction of W^{6+} ion to W^{5+} ions, and II to the reduction of W^{6+} and W^{5+} ions to W^{4+} ions. The activation energies for these two reduction processes are, within experimental error, the same (Table 2). The activation energy for the reduction of W^{4+} ions to W^0 (III) is considerably lower than for I and II, but is compensated for by a lower preexponential factor (A).

The tpr pattern of the 0.42 monolayer WO_3/Al_2O_3 sample (Fig. 5) shows only one broad reduction peak, which was assigned to the reduction of the amorphous tetrahedrally coordinated tungsten oxide species on the alumina. On the basis of the Raman observations, the shoulder at 1108 K observed for the monolayer sample was assigned to the reduction of WO_3 crystallites. The presence of WO_3 crystallites means that slightly in excess of a monolayer the tungsten oxide species is adsorbed under optimum equilibrium adsorption conditions. The formation of WO_3 crystallites can be due to a restructuring of the tungsten oxide monolayer, formed during adsorption, in the calcination process. No reduction in the BET surface area of the alumina was found upon calcination. It thus seems that calcination at 500°C alters the alumina surface in such a way that less tetrahedrally coordinated tungsten can be accommodated. XPS has shown that the reduction of tungsten oxide supported on alumina, at below monolayer coverages, does not take place via the lower oxidation states, W^{5+},

W^{4+}, and W^{2+}, but in a single step from the oxide to the metal (*11, 12*). This was explained in terms of a strong interaction between the tungsten oxide and the alumina, that prevents tungsten oxide crystallite formation, which is needed in order to stabilize the lower oxidation states (*11*). Our findings with tpr are in line with this as only one broad peak is observed for the 0.42 monolayer sample. However, the WO_3 crystallites present on the monolayer sample also appear to reduce in a single step. This could be due to their small crystallite size which must be <20 nm, as no WO_3 was observed with XRD.

The WO_3/TiO_2 profiles in Fig. 5 show that the reduction behavior of tungsten oxide supported on titania differs considerably from that supported on alumina. The reduction peaks at 1017 and 1248 K have been assigned to the reduction of the amorphous tetrahedrally coordinated tungsten oxide species. The peak at 655 K for the monolayer sample has been assigned to the reduction of WO_3 crystallites. The fact that the Raman spectra showed no WO_3 crystallites could be due to the following effect. TiO_2 has a weak Raman band at 794 cm^{-1} that could obscure the strongest WO_3 band at 808 cm^{-1}, which would be of very low intensity as only approximately 1.2% of the tungsten oxide is present as WO_3.

The fact that the 1017 K reduction peak corresponds to approximately 33% of the oxygen associated with the tungsten is a strong indication that this peak represents the $W^{6+} \rightarrow W^{4+}$ transition. This would mean that unlike alumina, titania can stabilize the W^{4+} oxidation state. The reason for the stabilizing effect of titania on W^{4+} becomes clear by comparing the physical properties of TiO_2 and WO_2 (Table 3). The ionic radius of W^{4+} and the W–O bond length are very similar to those for titania, and the crystal structure and unit cell of WO_2 are the same as for rutile. The following explanation for the two-step reduction of W^{6+} on TiO_2 can be put forward. After preparation of the WO_3/TiO_2 system by the equilibrium adsorption, the tungsten oxide and titania are already intimately contacted. During the tpr run the anatase TiO_2 is transformed to rutile while WO_3 is reduced to WO_2. The formed WO_2 can thus be immediately accommodated by the underlying rutile titania. It is also likely that some of the W^{4+} ions diffuse into the TiO_2 at higher temperatures, which would make these ions more difficult to reduce than those at the surface. Credence is given to this possibility by the fact that at monolayer coverage only 68% of the oxygen associated with the W^{4+} is removed.

TABLE 3

Physical Properties of WO_2 and TiO_2 (*21*)

Compound	Crystal symmetry class	Crystal structure	Ion radius (nm)	M–O bond length (nm)
TiO_2	Tetragonal	Anatase	0.068	0.195
TiO_2	Tetragonal	Rutile	0.068	0.194
WO_2	Tetragonal	Rutile	0.064	0.200

The onset of reduction in pure WO_3 is independent of sample size and starts at approximately 800 K (Fig. 3). For the titania and alumina supported WO_x, the onset of reduction is at 800 and 1100 K, respectively (Fig. 5). The higher reduction temperature needed for the reduction of the alumina-supported tungsten oxide, compared to that for the pure WO_3, is a clear indication that alumina has a stabilizing effect on the W^{6+} ions. A similar effect is not observed for titania. The activation energy for the reduction of W^{6+} to W^{4+} on titania is twice that for the same reduction in pure WO_3 (Table 2) and does indicate that the W^{6+} ions are stabilized by the titania. The fact that this is not observed in the tpr profiles is due to the much higher preexponential factor found for WO_3 on titania (Table 2), which compensates for the increase in activation energy. The increase in A may be explained by the surface reduction of titania, which takes place at 800 K (Fig. 5) and results in the formation of Ti^{3+} ions (*25*). These Ti^{3+}

ions could act as centers for catalytic H_2 dissociation and could thus catalyze the reduction of the supported tungsten. An increase in the concentration of catalytic centers for H_2 dissociation will explain the higher A value.

ACKNOWLEDGMENTS

The authors would like to acknowledge Sasol (Pty) Ltd. for financial support and thank Dr. M. E. Dry in particular.

REFERENCES

1. Ahmed, S. M., *J. Phys. Chem.* **73,** 3546 (1969).
2. Parfitt, G. D., *Pure Appl. Chem.* **48,** 415 (1976).
3. Wang, L., and Hall, W. K., *J. Catal.* **77,** 232 (1982).
4. Ng, K. T., and Hercules, D. M., *J. Phys. Chem.* **80,** 2094 (1976).
5. Salvati, L., Jr., Makovsky, L. E., Stencel, J. M., Brown, F. R., and Hercules, D. M., *J. Phys. Chem.* **85,** 3700 (1981).
6. Stencel, J. M., Makovsky, L. E., Diehl, J. R., and Sarkus, T. A., *J. Raman Spectrosc.* **15,** 282 (1984).
7. Chan, S. S., Wachs, I. E., Murrell, L. L., Wang, L., and Hall, W. K., *J. Phys. Chem.* **88,** 5831 (1984).
8. Horsley, J. A., Wachs, I. E., Brown, J. M., Via, G. H., and Hardcastle, F. D., *J. Phys. Chem.* **91,** 4014 (1987).
9. Thomas, R., and Moulijn, J. A., *J. Mol. Catal.* **15,** 157 (1982).
10. Thomas, R., van Oers, E. M., de Beer, V. H. J., Medema, J., and Moulijn, J. A., *J. Catal.* **76,** 241 (1982).
11. Wachs, I. E., Chersich, C. C., and Hardenbergh, J. H., *Appl. Catal.* **13,** 335 (1985).
12. Grünert, W., Shpiro, E. S., Feldhaus, R., Anders, K., Antoshin, G. V., and Minachev, Kh. M., *J. Catal.* **107,** 522 (1987).
13. Bond, G. C., Flamerz, S., and van Wijk, L., *Catal. Today* **1,** 229 (1987).
14. Soled, S., Murrell, L. L., Wachs, G. B., Sherman, L. G., Chan, S., Dispenziere, N. C., and Baker, R. T. K., *ACS Symp. Ser.* **279,** 165 (1985).
15. Ogata, E., Kamiya, Y., and Ohta, N., *J. Catal.* **29,** 296 (1973).
16. Gentry, S. J., Hurst, N. W., and Jones, A., *J. Chem. Soc. Faraday Trans. 1* **75,** 1688 (1979).
17. Knözinger, H., and Ratnasamy, P., *Catal. Rev. Sci. Eng.* **17,** 31 (1987).
18. Boehm, H. P., *in* "Advances Catalysis" (D. D. Eley, P. W. Selwood, and P. B. Weisz, Eds.), Vol. 16, p. 179. Academic Press, New York, 1966.
19. Pope, M. T., "Heteropoly and Isopoly Oxometalates." Springer-Verlag, Heidelberg, 1983.
20. Duncan, J. F., and Kepert, D. L., *J. Chem. Soc.*, 205 (1962); *J. Chem. Soc.*, 5317 (1969).
21. Krylov, O. V., "Catalysis by Non-Metals, Rules for Catalyst Selection." Academic Press, New York, 1970.
22. Hermann, M., and Boehm, H. P., *Z. Anorg. Allg. Chem.* **352,** 156 (1967).
23. Hermann, M., and Boehm, H. P., *Z. Anorg. Allg. Chem.* **368,** 73 (1969).
24. Arnoldy, P., de Jonge, J. C. M., and Moulijn, J. A., *J. Phys. Chem.* **89,** 4517 (1985).
25. Huizinga, T., and Prins, R., *J. Phys. Chem.* **85,** 2156 (1981).